

Consensus-based Frequency and Voltage Regulation for Fully Inverter-based Islanded Microgrids

Y. Cheng^{1,2}, Tao Liu^{1,2}

1. Department of Electrical and Electronic Engineering
The University of Hong Kong
Hong Kong SAR, China

2. Shenzhen Institute of Research and Innovation
The University of Hong Kong

David J. Hill^{3,4}

3. Department of Electrical and Electronic Engineering
The University of Hong Kong
Hong Kong SAR, China

4. School of Electrical Engineering and Telecommunications
University of New South Wales
Sydney, Australia

Xue Lyu

Department of Electrical and Computer Engineering
University of Wisconsin–Madison
Madison, USA

Abstract—This paper proposes a new distributed consensus-based control method for voltage and frequency control of fully inverter-based islanded microgrids (MGs). The proposed method includes the active power sharing in voltage control to improve the reactive power sharing accuracy and thus generalizes some existing secondary frequency and voltage control methods. Firstly, frequency is regulated by distributed secondary frequency control. Secondly, voltage is regulated by distributed average voltage control and decentralized individual voltage control. It offers a tunable trade-off between voltage regulation, active, and reactive power sharing accuracy. Therefore, it avoids the abuse of sacrificing reactive power sharing accuracy for exact voltage regulation which is a common issue of existing methods. The proposed method is implemented in a distributed way that does not require a prior knowledge of the MG network structure and loads and hence can ensure scalability. Simulation results show that the proposed controller achieves different compromise between the above three targets under different modes of operation.

Index Terms—Microgrid, power sharing, distributed consensus secondary control, voltage regulation, frequency regulation.

I. INTRODUCTION

Driven by the climate change and global warming, power systems are undergoing a significant transition. The core of this transition is to gradually replace fossil fuel based synchronous generators with renewable energy source-powered generators that are usually connected to the grid via converters, i.e., the converter interfaced generators (CIGs). The concept of MG plays an important role in connecting these CIGs, and thus attracts increasing attention recently. Usually, a MG consists of distributed generators such as wind turbines, solar panels, and microturbines [1] that are connected to the MG via inverters. Therefore, the control of a fully inverter-based islanded MG is of great importance.

Conventional $P-\omega$, $Q-V$ droop control method is the most popular primary control in fully inverter-based MGs since it

is simple to implement and does not require communication between CIGs. But its drawbacks cannot be neglected. Reference [2] summarizes these drawbacks. The most critical one is that it cannot accurately share reactive power among CIGs due to the mismatch in output impedance, which may cause circulating current among CIGs [2]–[7]. Some new control methods have been developed to address the issue, e.g., the $Q-\dot{V}$ droop control in [5] and the virtual impedance method in [4], [6]. These methods require *a priori* knowledge of the MG network. In addition, $P-V$, $Q-\omega$ droop control is also used in the literature due to the high R/X ratio of MGs [8].

On the other hand, droop control results in voltage and frequency deviations and thus secondary control methods are needed to restore their nominal values, e.g., [9]–[11]. However, many of the existing secondary voltage control methods aim at exact voltage regulation, i.e., restoring all CIG output voltage magnitude to a common reference value. [9], [11]. This may further deteriorate the reactive power sharing accuracy due to the fundamental conflict between voltage regulation and reactive power sharing [7]. To solve this issue, a tunable controller is proposed to achieve a balance between the accuracy in reactive power sharing and the performance in voltage regulation in [7]. Nevertheless, apart from reactive power, active power changes may also influence bus voltages in a MG due to its high R/X ratio and thus can be an alternative candidate to contribute to voltage regulation. To get active power in voltage regulation, trade-off between the accuracy in active power sharing and reactive power sharing, and the performance in voltage regulation should be considered simultaneously in the controller design of MGs to relax the burden of reactive power sharing accuracy.

Inspired by [7], this paper proposes a new tunable control method by including active power sharing in voltage regulation to achieve compromise among the three aforementioned control targets. We use reactive power control to regulate the frequency, and both active and reactive power control to regulate voltages. For the frequency regulation, we use the $Q-\omega$ droop control for the primary frequency control and a distributed sec-

This work was supported by the Research Grants Council of the Hong Kong Special Administrative Region under the General Research Fund through Project No. 17209219, and the National Natural Science Foundation of China through project No. 62173287.

ondary frequency control to restore the frequency to nominal value. For the voltage control, we offer an average voltage regulation and a triggered individual voltage regulation. The former is aimed to regulate average CIG voltage magnitude by controlling their active power output according to the active power sharing ratio. Only regulating average voltage may not be sufficient as individual CIG voltage magnitude may still be out of acceptable range. Therefore, we offer the triggered individual voltage regulation control method for each CIG to trigger when some preset conditions are satisfied, e.g., its output voltage is out of acceptable range. In individual voltage regulation, the active and reactive power output of that CIG is controlled without the consideration of power sharing ratio to regulate its output voltage magnitude.

The novelties of the proposed control method are threefold. Firstly, it can be implemented in distributed way and thus is scalable without requiring a *a priori* knowledge of the MG's network structure and loads. Secondly, the power sharing errors stemming from output impedance mismatch in conventional voltage droop control is solved by the proposed method where the corresponding power variable setpoints of CIGs, i.e., active power in this case, are determined via consensus-based control to achieve accurate power sharing. The CIGs' output voltage magnitudes are used to control to the desire power injection. This is different from voltage droop control where the output voltage magnitude follows the changes of power output. Effect of physical quantities of the MG, i.e., output impedance, in power sharing in voltage droop control is eliminated as the consensus is reached on communication level. Thirdly, it generalizes the methods proposed in [7], [9]–[11] to achieve a trade-off between the aforementioned three control targets. In particular, it extends the ideas in [7] to include the accuracy of active power sharing in the trade-off to prevent abusing the reactive power sharing accuracy.

The rest of the paper is organized as follows. Section II introduces the system model. In section III, the proposed control method is introduced and its performance is demonstrated in Section IV. Conclusions are given in Section V.

II. MODEL DESCRIPTION

We consider a MG with n buses and m distribution lines with $\mathcal{N} = \{1, \dots, n\}$, $\mathcal{M} = \{1, \dots, m\}$ as the corresponding index sets. We divide all buses in the MG into three types: a CIG bus, a load bus, and an intermediate bus that refers to a bus that has no CIGs and loads. We denote the index set of CIG buses as $\mathcal{C} = \{1, 2, \dots, c\}$, and load bus as $\mathcal{L} = \{c+1, \dots, l\}$, where c and l are the number of CIGs and loads in the MG respectively. For simplicity, we assume $\mathcal{C} \cap \mathcal{L} = \emptyset$ and the MG has at least one CIG, one line, and one load.

Here we only consider a three-phase balanced MG. We apply Park transformation to transform three-phase balanced signals into the direct and quadrature (d – q) axes components. We denote the CIG at bus i , $i \in \mathcal{C}$, as CIG_i and its model is built under the $d_i - q_i$ frame at its local frequency ω_i . For each line j , $j \in \mathcal{M}$ and each load bus h , $h \in \mathcal{L}$, their models are built under the system $D - Q$ frame at

the nominal frequency ω_s . To form the whole network, we change a CIG variable x_i^{dq} under the $d_i - q_i$ frame to that X_i^{DQ} under the $D - Q$ frame by a transformation T_i , i.e., $X_i^{DQ} = T_i x_i^{dq}$ and $x_i^{dq} = T_i^{-1} X_i^{DQ}$ with $x_i^{dq} = (x_i^d, x_i^q)^\top$, $X_i^{DQ} = (X_i^D, X_i^Q)^\top$, [4], [12]. The transformation matrix T_i is defined as:

$$T_i = \begin{pmatrix} \cos \delta_i & -\sin \delta_i \\ \sin \delta_i & \cos \delta_i \end{pmatrix} \quad (1)$$

with $\delta_i = \omega_i - \omega_s$.

The superscripts dq and DQ denote that the rated variables are defined under the $d_i - q_i$ and $D - Q$ frame respectively. The whole MG model consists of differential algebraic equations. The differential equations are used to represent dynamics of CIGs, lines, and loads are described below.

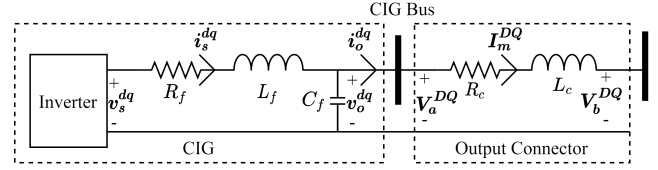


Fig. 1. Configuration of a CIG and its output connector.

A. CIG Model

Here, we adopt the configuration of CIGs as that in [9]–[12]. For simplicity, we neglect the DC-side dynamics for simplicity, and adopt the assumption therein that each CIG connects to the MG via an output connector which is modelled as a distribution line with resistance R_c and inductance L_c . The configuration of the CIG and its output connector is shown in Fig. 1, where the switching voltage $v_{s_i}^{dq}$ and frequency ω_i are considered as input variables, which will be designed later. The mathematical model of CIG_i with the switching current $i_{s_i}^{dq}$ and $v_{o_i}^{dq}$ as its states are given as follows [9]–[12]:

$$\dot{i}_{s_i}^{dq} = L_{f_i}^{-1} (-R_{f_i} i_{s_i}^{dq} + v_{s_i}^{dq} - v_{o_i}^{dq}) + \omega_i K i_{s_i}^{dq} \quad (2)$$

$$\dot{v}_{o_i}^{dq} = C_{f_i}^{-1} (i_{s_i}^{dq} - i_{o_i}^{dq}) + \omega_i K v_{o_i}^{dq} \quad (3)$$

where $K = \begin{bmatrix} 0 & 1 \\ -1 & 0 \end{bmatrix}$; R_{f_i} , L_{f_i} , C_{f_i} are the output filter's resistance, inductance, and capacitance of CIG_i , respectively.

B. Distribution Line Model

For a distribution line m , $m \in \mathcal{M}$, that connects bus a and b with $a, b \in \mathcal{N}$, we model it as a RL circuit with a series resistance R_m and inductance L_m . The dynamics of the current I_m^{DQ} going through the line is [12]:

$$\dot{I}_m^{DQ} = L_m^{-1} (-R_m I_m^{DQ} + V_a^{DQ} - V_b^{DQ}) + \omega_s K I_m^{DQ} \quad (4)$$

where V_a^{DQ} and V_b^{DQ} are the bus voltages at bus a and b , respectively.

C. Load Model

We assume that the load at bus h , $h \in \mathcal{L}$, is a series RL load with a resistance R_{load_h} and inductance L_{load_h} . The dynamics of the current, \mathbf{i}_h^{DQ} , going through the load is [12]:

$$\dot{\mathbf{i}}_h^{DQ} = L_{load_h}^{-1} (-R_{load_h} \mathbf{i}_h^{DQ} + \mathbf{V}_h^{DQ}) + \omega_s K \mathbf{i}_h^{DQ}. \quad (5)$$

Note that the voltage at the load bus, \mathbf{V}_h^{DQ} , can be calculated by solving the algebraic equation established by Kirchhoff's Current Law (KCL) at the load bus h .

Different components are connected together by applying KCL at every buses to establish the algebraic equations of the whole network.

III. PROPOSED CONTROL METHOD

The proposed control method is aimed to regulate the frequency, voltage, and power sharing accuracy by controlling CIG_i output frequency ω_i , its reactive power output Q_i , and active power output P_i . The setpoint P_i^* of P_i is the sum of three variables, i.e., the nominal active power output P_i^{nom} , the active power P_i^{Vav} to regulate average CIG output magnitude $\|\bar{v}_o\|$, and the active power P_i^{Vind} to regulate individual CIG_i output voltage magnitude $\|\mathbf{v}_{o_i}^{dq}\|$.

For frequency regulation, $Q - \omega$ droop control and its associated distributed secondary frequency control are used. For voltage regulation, it offers the average voltage regulation and individual voltage regulation. In average voltage regulation, distributed consensus algorithm is implemented to give an estimation of average CIG_i voltage magnitude, $\|\bar{v}_o\|$, to each CIG_i . Then, CIG_i calculates P_i^{Vav} based on predefined active power sharing ratio to regulate $\|\bar{v}_o\|$. As accurate power sharing conflict with exact voltage regulation, only exact average voltage regulation can be achieved with accurate power sharing. If individual voltage regulation is required, i.e., even when average voltage magnitude equals to nominal value, we still require the output voltage magnitude of a CIG to get closer to nominal value or even be equal to nominal value, then the power output of that CIG needs to change without considering power sharing ratio. Therefore, in individual voltage regulation, CIG_i calculates P_i^{Vind} and Q_i^{Vind} regardless of power sharing ratio to control P_i and Q_i to regulate $\|\mathbf{v}_{o_i}^{dq}\|$. Summing P_i^{nom} , P_i^{Vav} , and P_i^{Vind} , the setpoint P_i^* of P_i is obtained. Then a cascaded inner control loop is implemented to calculate the control input to CIG_i , i.e., the switching voltage, to inject the desired active power to MG. Fig 2. shows the control block diagram of the proposed control method. We assume P_i^{nom} and Q_i^{nom} are selected based on the predefined power sharing ratio.

The instantaneous active power output P_i , reactive power output Q_i , and output voltage magnitude $\|\mathbf{v}_{o_i}^{dq}\|$ of CIG_i are calculated as follows:

$$P_i = v_{o_i}^d i_{o_i}^d + v_{o_i}^q i_{o_i}^q, Q_i = v_{o_i}^q i_{o_i}^d - v_{o_i}^d i_{o_i}^q, \quad (6)$$

$$\|\mathbf{v}_{o_i}^{dq}\| = \sqrt{(v_{o_i}^d)^2 + (v_{o_i}^q)^2}. \quad (7)$$

A. Primary Frequency Control: $Q - \omega$ Droop Control

The output frequency ω_i of CIG_i is controlled as follows [13]:

$$Q_i^{base} = Q_i^{nom} + Q_i^{Vind} \quad (8)$$

$$\omega_i = \omega_i^* + m_i(Q_i - Q_i^{base}) \quad (9)$$

where Q_i^{base} is the reactive power output base value and is the sum of the nominal reactive power base value Q_i^{nom} and reactive power Q_i^{Vind} to regulate individual CIG_i output voltage magnitude. ω_i^* is the frequency setpoint to be determined in section III-B; m_i is the frequency droop coefficient of CIG_i . $Q - \omega$ droop control results in frequency deviation and thus distributed secondary frequency control is used to control it back to ω_s by controlling ω_i^* .

B. Distributed Secondary Frequency Control

We assume that there exists a bidirectional connected communication network between CIGs. We denote its network topology as an undirected graph \mathcal{G} . We use $A \in \mathbb{R}^{c \times c}$ to denote the adjacency matrix of \mathcal{G} with all edge weights equal to one and a_{ij} denotes the (i, j) th entry of A . We assume the communication between CIGs is periodic with a period t_1 , i.e., at every t_1 seconds, each CIG_i sends its current output frequency $\hat{\omega}_{i,k_1} = \omega_i(k_1 t_1)$, reactive power sharing signals $\hat{Q}_{i,k_1} = m_i(Q_i(k_1 t_1) - Q_i^{base}(k_1 t_1))$ with $k_1 = 0, 1, 2, \dots$ to its communication neighbours. As Q_i^{base} is included in the droop control, the distributed secondary frequency control in [8] is modified accordingly and the local setpoint ω_i^* of CIG_i is calculated as follows:

$$\begin{aligned} \hat{\omega}_i^* = & -c_f(b_i(\omega_i - \omega_s) + \sum_{j \in \mathcal{N}_i} a_{ij}(\omega_i - \hat{\omega}_{j,k_1} \\ & - m_i Q_i + \hat{Q}_{j,k_1})) \end{aligned} \quad (10)$$

where \mathcal{N}_i is the index set of communication neighbours of CIG_i ; c_f and b_i are the the coupling gain and pinning gain, respectively. We assume $b_i \geq 0$ is non-zero for only one selected CIG. The distributed secondary frequency control was originally proposed in [10] for $P - \omega$ droop. Here, we modified it for the $Q - \omega$ droop [8], [10] in (10). The term $a_{ij}(\omega_i - \hat{\omega}_{j,k_1}) + b_i(\omega_i - \omega_s)$ is the tracking error of frequency while $a_{ij}(-m_i(Q_i - Q_i^{base}) + \hat{Q}_{j,k_1})$ is the tracking error of reactive power sharing. Their convergence speed can be adjusted independently by assigning two different gains but here we use a common coupling gain c_f for simplicity. The term $b_i(\omega_i - \omega_s)$ is to ensure that one CIG has access to ω_s and its local frequency is tracked with ω_s with the tracking rate determined by b_i .

C. Active Power Control

The aim of active power control is to regulate the active power output of CIG_i P_i to its setpoint P_i^* which consists of three components, i.e., P_i^{nom} , P_i^{Vav} , and P_i^{Vind} . In the rest of the paper, we use K_p and K_i to denote the proportional gain and integral gain of a PI controller respectively with different

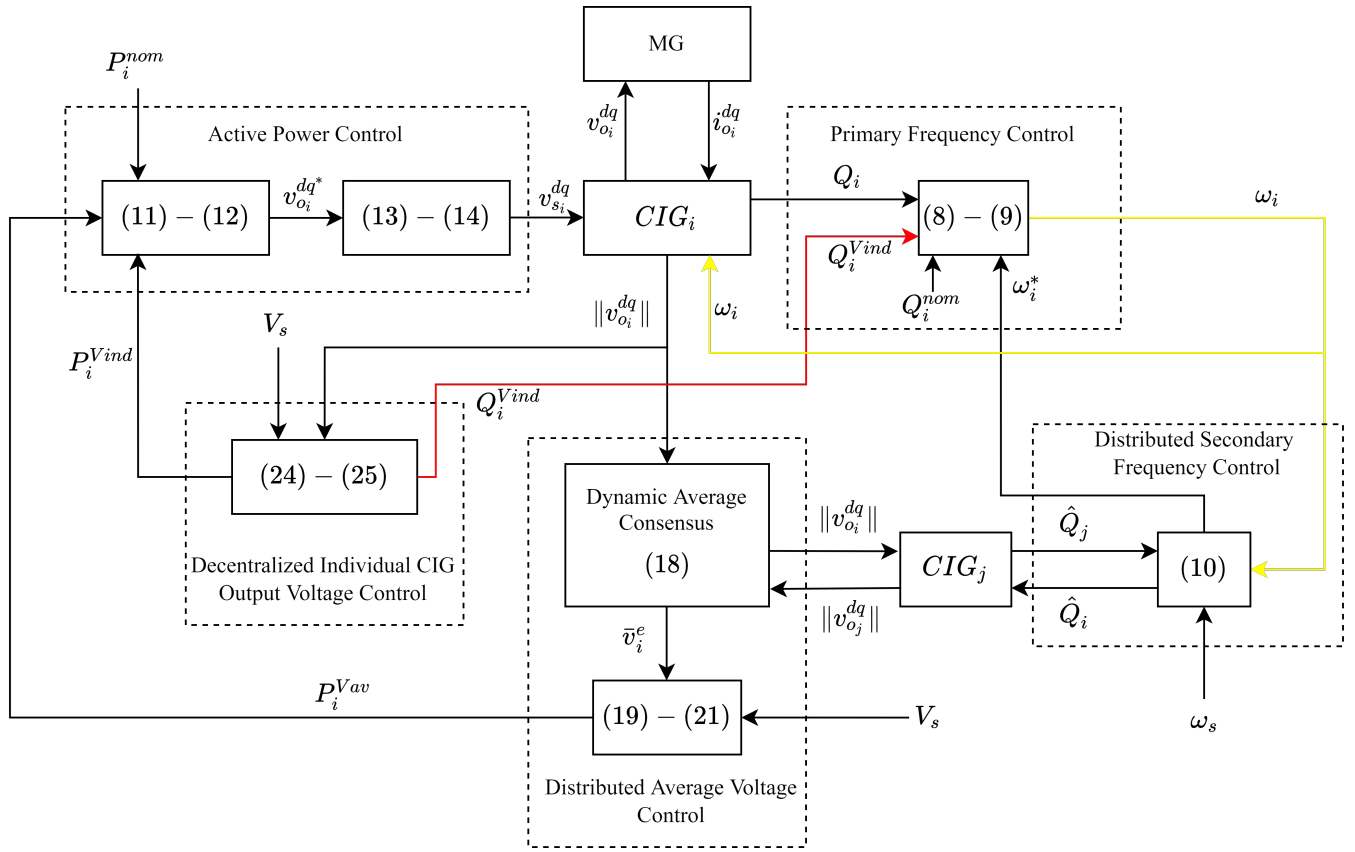


Fig. 2. Control block diagram of proposed controller

superscripts representing different PI controllers. The setpoint P_i^* , $v_{o_i}^d$ setpoint $v_{o_i}^{d*}$ are calculated as follows:

$$P_i^* = P_i^{nom} + P_i^{Vav} + P_i^{Vind} \quad (11)$$

$$v_{o_i}^{d*} = K_p^{vd}(v_{o_i}^{dset} - v_{o_i}^d) + K_i^{vd} \int_0^t (v_{o_i}^{dset} - v_{o_i}^d) dt. \quad (12)$$

The control variable $v_{o_i}^{dset}$ is defined as $v_{o_i}^{dset} = \text{sgn}(i_{o_i}^d) \frac{P_i^*}{(|i_{o_i}^d| + \varepsilon)}$, where ε is a small positive constant to avoid $v_{o_i}^{dset}$ going to infinity; $\text{sgn}(i_{o_i}^d) = 1$ for $i_{o_i}^d \geq 0$ and $\text{sgn}(i_{o_i}^d) = -1$ otherwise. $v_{o_i}^q$ setpoint $v_{o_i}^{q*}$ is set to zero. The $v_{o_i}^{dq}$ setpoint $v_{o_i}^{dq*}$ are then used to calculate the control input, i.e., switching voltage $v_{s_i}^{dq}$, of CIG_i as follows to regulate $v_{o_i}^{dq}$ to $v_{o_i}^{dq*}$ [9], [11], [12]:

$$\begin{aligned} i_{s_i}^{dq*} = & F i_{o_i}^{dq} - C_f \omega K v_{o_i}^{dq} + K_p^v (v_{o_i}^{dq*} - v_{o_i}^{dq}) \\ & + K_i^v \int_0^t (v_{o_i}^{dq*} - v_{o_i}^{dq}) dt \end{aligned} \quad (13)$$

$$\begin{aligned} v_{s_i}^{dq} = & -L_f \omega K i_{s_i}^{dq} + K_p^i (i_{s_i}^{dq*} - i_{s_i}^{dq}) \\ & + K_i^i \int_0^t (i_{s_i}^{dq*} - i_{s_i}^{dq}) dt \end{aligned} \quad (14)$$

where F is the current feed forward gain.

D. Distributed Average Voltage Control

We regulate $\|\bar{v}_o\|$ by controlling P_i^{Vav} based on predefined active power sharing ratio. The following shows the correlation between P_i and $\|\bar{v}_o\|$ in steady state.

The active power flow equation of CIG_i in bus i is as follows:

$$P_i = \|V_i\| \|V_j\| (-G \cos(\theta_i - \theta_j) - B \sin(\theta_i - \theta_j)) + G \|V_i\|^2 \quad (15)$$

where $\|V_i\|$ and θ_i are the voltage magnitude and phase angle of bus i , respectively; G and B are the conductance and susceptance of output connector.

Taking the partial derivative of P_i with respect to $\|V_i\|$, we have the following:

$$\frac{\partial P_i}{\partial \|V_i\|} = \frac{P_i + G \|V_i\|^2}{\|V_i\|}. \quad (16)$$

As $P_i \geq 0$, $G > 0$ and $\|V_i\|^2 \geq 0$, we can conclude that P_i has a positive correlation with $\|V_i\|$, i.e., $\|v_{o_i}^{dq}\|$.

The following shows the definition of $\|\bar{v}_o\|$:

$$\|\bar{v}_o\| = \frac{1}{c} \sum_{i=1}^c \|v_{o_i}^{dq}\|. \quad (17)$$

It can be easily conclude that P_i has a positive correlation with $\|v_{o_i}^{dq}\|$ and thus $\|\bar{v}_o\|$.

If every CIG_i knows $\|\bar{v}_o\|$ and changes their P_i based on $\|\bar{v}_o\|$ and predefined active power sharing ratio to regulate $\|\bar{v}_o\|$, then $\|\bar{v}_o\|$ can be driven to nominal CIG output voltage magnitude, V_s , while maintaining accurate active power sharing among CIGs. Thus, dynamic average consensus algorithm is implemented to give an estimation $\|\bar{v}_o\|$ in the MG to each CIG_i . At every sampling time $k_2 t_2$ with $k_2 = 0, 1, 2, \dots$ and $t_2 > t_1$, CIG_i sets the input u_{i,k_2} to the consensus algorithm as $\|\mathbf{v}_{o_i}^{dq}(k_2 t_2)\|$ and fixes it during that sampling time interval. CIG_i communicates every t_1 seconds and the state variable r_i and the agreement state x_i of CIG_i are calculated as follows [14]:

$$r_{i,k_1+1} = (1 + \rho^2)r_{i,k_1} - \rho^2 r_{i,k_1-1} + k_I \sum_{j=1}^N a_{ij}(x_{i,k_1} - x_{j,k_1}) \quad (18)$$

where $x_{i,k_1} = u_{i,k_2} - r_{i,k_1}$, ρ and k_I are parameters. $r_{i,0}$ is initialized as zero to satisfy to requirement of the average of initial integrator states equal to zero [14]. At sampling time $k_2 t_2$, x_{i,k_1} is considered as the estimation of average inverter bus voltage magnitude \bar{v}_{i,k_2} for CIG_i first and then u_{i,k_2} is updated with $\|\mathbf{v}_{o_i}^{dq}(k_2 t_2)\|$.

The active power contribution of CIG_i in regulating $\|\bar{v}_o\|$, P_i^{Vav} , which is a component of P_i^* , is controlled by the discrete PI controller with the compensator formula $K_p^A + K_i^A \frac{t_2}{z-1}$ and sample time t_2 as follows:

$$e_{i,k_2} = V_n - \bar{v}_{i,k_2}^e \quad (19)$$

$$d_{i,k_2} = d_{i,k_2-1} + K_p^A(e_{i,k_2} - e_{i,k_2-1}) + K_i^A(t_2 \cdot e_{i,k_2-1}) \quad (20)$$

$$P_i^{Vav} = n_i d_{i,k_2} \quad (21)$$

where n_i denote the P_i^{Vav} sharing gain of CIG_i . As long as every CIG receives the same \bar{v}_{i,k_2}^e signal, i.e., consensus is reached, the responsibility of regulating $\|\bar{v}_o\|$ via active power can be shared accurately based on n_i . The number of iterations needed for the average consensus error to be smaller than certain threshold depends on the topology of the communication network. Thus, t_2 can be determined based on t_1 and the acceptable P_i^{Vav} sharing error. [14] provides detailed analysis of the convergence rate of the above algorithm and the rules of choosing optimal parameters.

E. Decentralized Individual CIG Output Voltage Control

Decentralized individual CIG output voltage control is a triggered control function for individual CIG and is triggered under some preset conditions, e.g., the $\|\mathbf{v}_{o_i}^{dq}\|$ is out of acceptable range. Two variables, P_i^{Vind} and Q_i^{Vind} , are controlled to vary P_i and Q_i to regulate $\|\mathbf{v}_{o_i}^{dq}\|$. As mentioned before, the accurate power sharing and individual $\|\mathbf{v}_{o_i}^{dq}\|$ voltage regulation conflict with each other. Therefore, the predefined power sharing ratio is not considered in individual $\|\mathbf{v}_{o_i}^{dq}\|$ voltage regulation, i.e., P_i^{Vind} and Q_i^{Vind} are calculated without taking the power sharing ratio into account. When it is triggered, $\|\mathbf{v}_{o_i}^{dq}\|$ is regulated and the power sharing accuracy

is not guaranteed. When it is not triggered, P_i^{Vind} and Q_i^{Vind} are set to zero and power sharing accuracy is preserved.

The positive correlation between P_i and $\|\mathbf{v}_{o_i}^{dq}\|$ has been shown in (16) and the correlation between Q_i and $\|\mathbf{v}_{o_i}^{dq}\|$ in steady state is showed as the following.

The reactive power flow equation of CIG_i in bus i is as follows:

$$Q_i = \|V_i\| \|V_j\| (-G \sin(\theta_i - \theta_j) + B \cos(\theta_i - \theta_j)) - B \|V_i\|^2 \quad (22)$$

Taking the partial derivative of Q_i with respect to $\|V_i\|$, we have the following:

$$\frac{\partial Q_i}{\partial \|V_i\|} = \frac{Q_i - B \|V_i\|^2}{\|V_i\|}. \quad (23)$$

Since the loads and distribution lines in MGs are usually inductive rather than capacitive, Q_i is usually larger than zero if CIGs share the reactive power properly. As $Q_i \geq 0$, $B < 0$ and $\|V_i\|^2 \geq 0$, we conclude that Q_i has a positive correlation with $\|V_i\|$, i.e., $\|\mathbf{v}_{o_i}^{dq}\|$. Even if $Q_i < 0$, the term $-B \|V_i\|^2$ may still make $Q_i - B \|V_i\|^2$ be positive. Note that B is the susceptance of the output connector. By choosing B properly, $Q_i - B \|V_i\|^2 > 0$ generally holds and thus Q_i is still positively correlated with $\|\mathbf{v}_{o_i}^{dq}\|$.

Given the positive correlation between CIG_i power injection and $\|\mathbf{v}_{o_i}^{dq}\|$, individual $\|\mathbf{v}_{o_i}^{dq}\|$ is regulated by controlling P_i^{Vinv} , which is one of the component of P_i^* , and Q_i^{Vind} , which is one of the component of Q_i^{base} , as follows:

$$P_i^{Vind} = K_p^P (V_s - \|\mathbf{v}_{o_i}^{dq}\|) + K_i^P \int_0^t (V_s - \|\mathbf{v}_{o_i}^{dq}\|) dt \quad (24)$$

$$Q_i^{Vind} = K_p^Q (V_s - \|\mathbf{v}_{o_i}^{dq}\|) + K_i^Q \int_0^t (V_s - \|\mathbf{v}_{o_i}^{dq}\|) dt. \quad (25)$$

The proportional gains and integral gains determine the extent of sacrificing the accuracy in active and reactive power sharing in the trade-off with individual $\|\mathbf{v}_{o_i}^{dq}\|$ regulation. P_i^{Vind} and Q_i^{Vind} are the stems of power sharing errors. The following is the two modes of operation.

1) *Partial Individual $\|\mathbf{v}_{o_i}^{dq}\|$ Control*: Integral gains are set to zero with at least one proportional gain being greater than zero. Trade-off between the accuracy in power sharing and individual $\|\mathbf{v}_{o_i}^{dq}\|$ regulation is determined by the value of K_p^P and K_p^Q . Individual $\|\mathbf{v}_{o_i}^{dq}\|$ is not driven to V_s due to the absence of the integral action.

2) *Exact Individual $\|\mathbf{v}_{o_i}^{dq}\|$ Control*: At least one integral gain is greater than zero. Individual $\|\mathbf{v}_{o_i}^{dq}\|$ is driven to V_s due to the integral action. If K_i^P and K_p^P are set to zero and K_i^Q is larger than zero, the performance of the controller will be very similar to those in [9]–[11], i.e., the active power is accurately shared and the accuracy in reactive power sharing is traded off with the exact individual $\|\mathbf{v}_{o_i}^{dq}\|$ regulation.

Remark 1: $Q - f$ instead of $P - f$ is used since we would like to control active power, P , as a non-slack variable for better coordination with primary energy source. Existing methods usually control P as a slack variable and assume the

primary energy source can supply active power instantaneously to regulate dc link voltage, which is not necessarily true. In the proposed control method, the output voltage magnitude and reactive power are slack variables. The amount of P injection is directly controlled.

Remark 2: Since distributed lines and loads are modelled as RL circuits, their active power consumption are voltage sensitive (their voltage depends on the active power supplied to them). As P is a non-slack variable while reactive power, Q , is a slack variable, the most direct way to regulate average voltage is to control the P setpoint of each CIG according to the active power sharing ratio. When the P injection from a CIG changed, its Q injection changes accordingly and may violate the Q sharing ratio among CIGs. However, the error in Q sharing is then eliminated by the $Q - f$ droop control.

IV. CASE STUDY

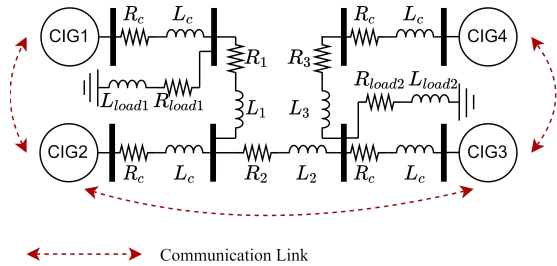


Fig. 3. Microgrid Test System.

A test system originally from [11] is modified for case study in this section. The digram of the test system is shown in Fig. 3. Four cases are simulated to compare the performance of the proposed control methods with the method used in [10], [11] with the $P - f$, $Q - V$ droop control and secondary control (PFQV). Three different cases of the proposed control methods are used from case 1 to case 3, respectively. PFQV is implemented in case 4. Note that we assume continuous communication between CIGs in PFQV. This is different from case 1 to 3 where only discrete communication is used to demonstrate the robustness of the proposed controller. Besides, only one CIG in PFQV can access V_s in PFQV but in the proposed control method we assume all CIGs know V_s . This assumption is valid as V_s is usually defined in grid code and seldom changes.

From case 1 to case 3, Q_i^{nom} is set to 0Var and P_i^{nom} is linearly increased from 0W to 20000W in first 3s in all CIGs. The power sharing gains m_i and n_i in all CIGs in each method are set to be the same to share the power equally among CIGs, i.e., the active and reactive power from each CIG should be the same ideally. In case 4, the droop gains in $P - f$ and $Q - V$ droop in all CIGs are set to be identical with each other as well. Therefore, their power sharing performance can be evaluated by observing whether the active and reactive power output from each CIG are the same. V_s is chosen as 400V and two step load change occur at 35s in load1 and 50s

in load2, respectively, in all cases. t_1 and t_2 are chosen as 0.025s and 0.05s, respectively.

From case 1 to case 3, the PI controller of P_i^{Vav} is activated at 5s and the dynamic consensus algorithm is activated at 0s. For the decentralized individual CIG output voltage control, it is not triggered in case 1; mode 1 ($K_p^P = K_p^Q = 1000$) and mode 2 ($K_p^P = K_p^Q = 1000$, $K_i^P = 2000$, $K_i^Q = 1500$) are triggered in all CIGs at 20s in case 2 and case 3, respectively. Therefore, the control actions from case 1 to 3 are the same before 20s and the results overlap with each other. In case 4, both secondary frequency and voltage control are activated at 5s.

TABLE I
COMPARISON OF TRADEOFF OF BETWEEN
DIFFERENT OBJECTIVES IN FOUR CASES

Case	Sacrifice of P Sharing Accuracy	Sacrifice of Q Sharing Accuracy	Voltage Regulation Extent
1	No	No	Average Voltage Control
2	Yes, via proportional control in (24)	Yes, via proportional control in (25)	Average Voltage Control with Partial Individual $\ v_{o_i}^{dq}\ $ Control
3	Yes, via proportional and integral control in (24)	Yes, via proportional and integral control in (25)	Average Voltage Control with Exact Individual $\ v_{o_i}^{dq}\ $ Control
4	No	Yes	Exact Voltage Regulation

A. Frequency

Fig. 4 compares the frequency regulation performance in four cases. Their frequency regulation performance is similar with each other as the principle of secondary frequency control used is the same. The differences are that $Q - f$ primary droop control is used in case 1 to 3 while $P - f$ primary droop control is used in case 4 and the base value in $Q - f$ primary droop control in case 2 and 3 started to change at 20s due to the decentralized individual CIG output voltage control, resulting in large disturbance in frequency at 20s.

B. Voltage Regulation

Fig. 5 compares the output voltage magnitude of CIGs in four cases. In case 1, only the average of output voltage magnitude is regulated to 400V. Individual CIG output voltage magnitude is not regulated. In case 2, individual CIG output voltage magnitude is partially regulated as we can see each CIG output voltage magnitude is closer to 400V than that in Case 1 after enabling the partial individual $\|v_{o_i}^{dq}\|$ control at 20s. In case 3, individual CIG output voltage magnitude is exactly regulated to 400V after enabling the exact individual $\|v_{o_i}^{dq}\|$ control at 20s. In case 4, individual CIG output voltage magnitude is exactly regulated to 400V after the secondary voltage control in [10], [11] is enabled at 5s. Noted that the voltage in case 4 is regulated more tightly than that in case 3 under step load changes. By selecting larger proportional

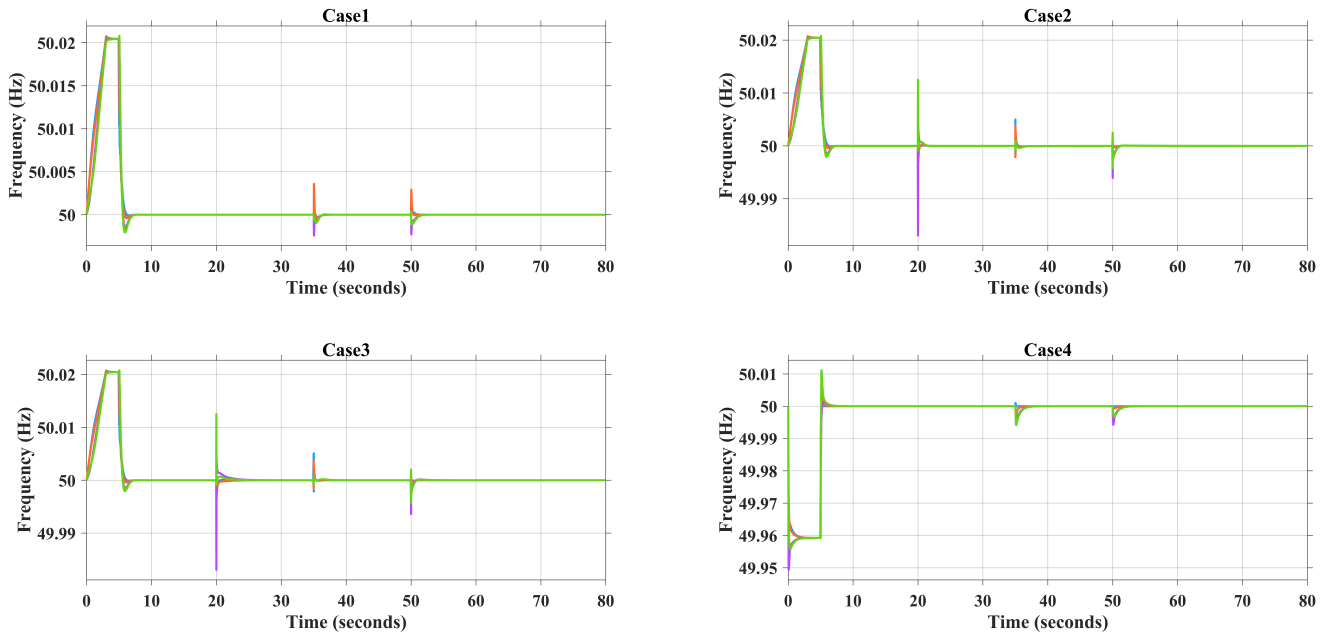


Fig. 4. Frequency. Blue: CIG1. Orange: CIG2. Purple: CIG3. Green: CIG4.

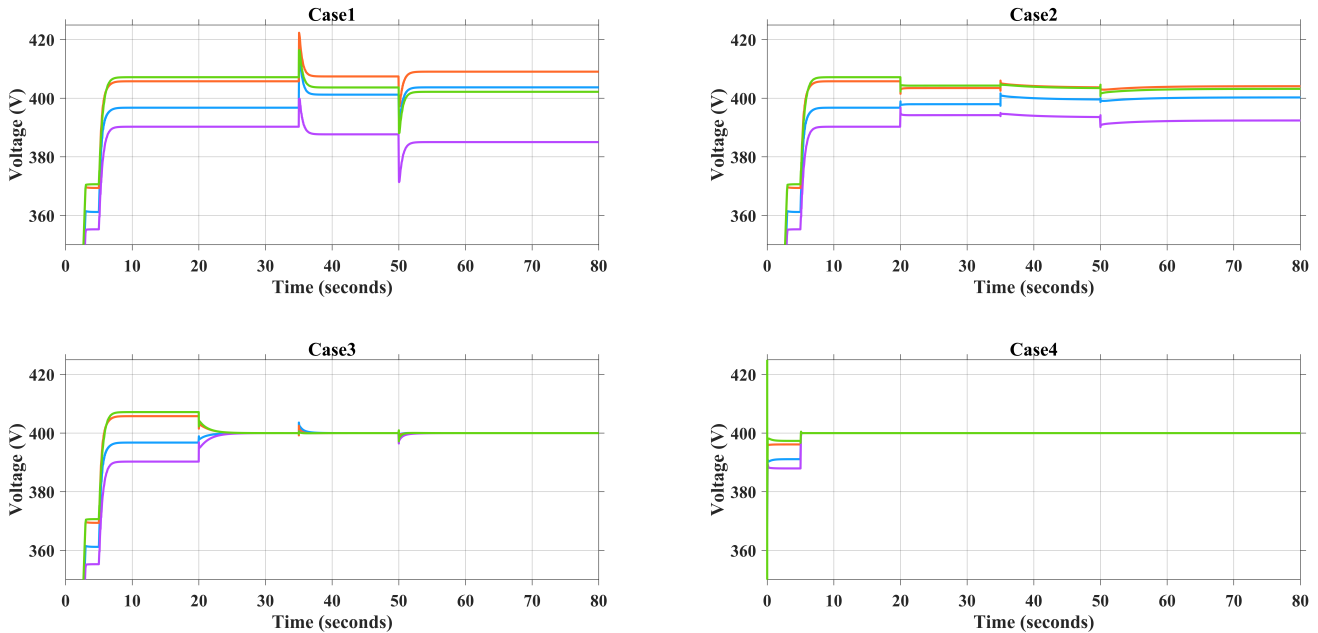


Fig. 5. Output voltage magnitude. Blue: CIG1. Orange: CIG2. Purple: CIG3. Green: CIG4.

gain and integral gain in decentralized individual CIG output voltage control, the voltage can be regulated more tightly in our proposed method. However, this may deteriorate the frequency regulation performance as the base value in the primary droop control is changed faster.

C. Active Power

Fig. 6 compares the active power injection of CIGs in four cases. The order of active power sharing accuracy is : Case 1 = Case 3 > Case 2 > Case 3.

D. Reactive Active Power

Fig. 7 compares the reactive power injection of CIGs in four cases. The order of active power sharing accuracy is : Case 1 > Case 2 > Case 3 > Case 4.

E. Summary

Table II summarizes the tradeoff in control performance between active power sharing accuracy, reactive power sharing accuracy and exactness of voltage regulation in different cases. It can be observed in Fig. 6 and Fig. 7 that the nearest CIG

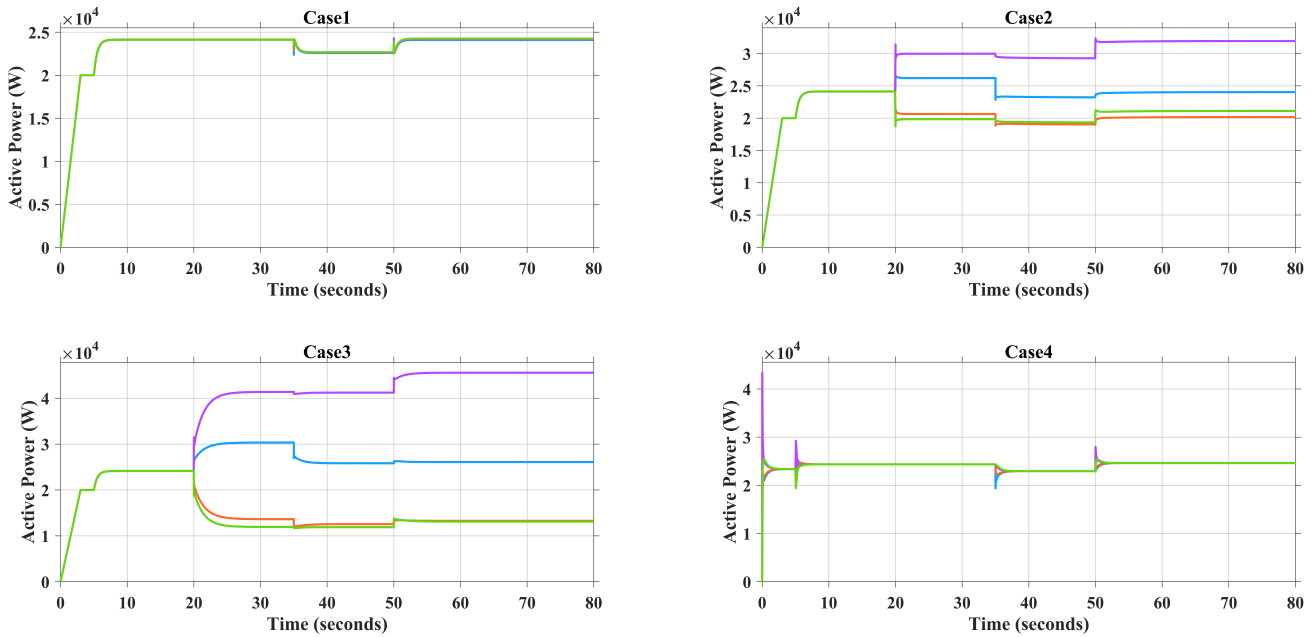


Fig. 6. Active power injection. Blue: CIG1. Orange: CIG2. Purple: CIG3. Green: CIG4.

TABLE II
COMPARISON OF RELATIVE CONTROL PERFORMANCE IN DIFFERENT PARAMETERS IN FOUR CASES

Case	Frequency Regulation	P Sharing Accuracy	Q Sharing Accuracy	Exactness of Voltage Regulation
1	same	✓✓✓	✓✓✓✓	✓
2	same	✓✓	✓✓✓	✓✓
3	same	✓	✓✓	✓✓✓
4	same	✓✓✓	✓	✓✓✓

¹The number of ✓ only represents the relative control performance of that case on that parameter. It does not represent the relative performance across different parameters.

with respect to the load change reacts most if the control method cannot share active or reactive power accurately, i.e., when load 1 changes at 35s, CIG 1 power output (the blue lines) changes most. When load 2 changes at 50s, CIG 3 power output (the purple lines) changes most.

In practice, voltage regulation performance without decentralized individual CIG output voltage control (case 1) usually satisfies the voltage regulation requirement. Given a set of predefined active and reactive power sharing ratio among CIGs, exact voltage regulation may not always be possible. If exact voltage regulation is needed, the accuracy of power sharing has to be sacrificed. Different from existing controllers where the only choice to be sacrificed is reactive power sharing accuracy, the proposed controller allows the possibility sacrifice of active power sharing accuracy such that a balance can be stroked. Only sacrificing reactive power accuracy may lead to overloading of a particular CIG and high

circulating current among CIGs.

Voltage may be more sensitive to active power change than reactive power change due to the high R/X ratio in MG [1], [8], [11], i.e., a small active power change may have the same effect on voltage as a large reactive power change. Hence, active power should also be considered in voltage regulation.

V. CONCLUSION

In this paper, we have proposed a tunable distributed secondary voltage and frequency regulation controller with controllable compromise between power sharing accuracy and voltage regulation. Different modes of operation has been demonstrated in the test system. Our case studies has shown that: 1) the proposed new control paradigm can overcome the inaccuracy in power sharing in conventional voltage droop meanwhile achieving accurate $\|\bar{v}_o\|$ regulation (case 1); 2) trade-off between active power sharing accuracy, reactive power sharing accuracy and voltage regulation performance is achieved (case 2 and 3); 3) reactive power sharing accuracy can be improved by including active power sharing in the trade-off (case 3 and 4). Future works will be done on choosing optimal parameters in the proposed controller.

REFERENCES

- [1] D. E. Olivares, A. Mehrizi-Sani, A. H. Etemadi, C. A. Cañizares, R. Iravani, M. Kazerani, A. H. Hajimiragha, O. Gomis-Bellmunt, M. Saeedifard, R. Palma-Behnke, G. A. Jiménez-Estévez, and N. D. Hatziargyriou, "Trends in microgrid control," *IEEE Transactions on Smart Grid*, vol. 5, no. 4, pp. 1905–1919, July 2014.
- [2] M. Eskandari, L. Li, M. H. Moradi, P. Siano, and F. Blaabjerg, "Active power sharing and frequency restoration in an autonomous networked microgrid," *IEEE Transactions on Power Systems*, vol. 34, no. 6, pp. 4706–4717, Nov 2019.

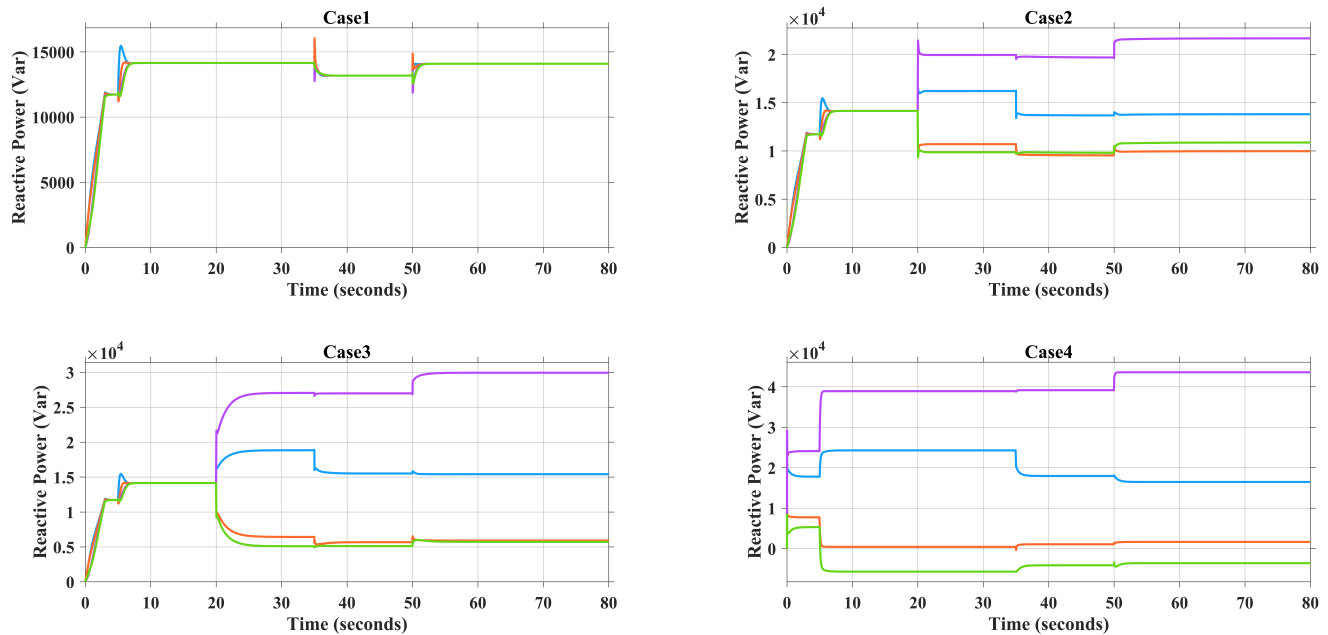


Fig. 7. Reactive power injection. Blue: CIG1. Orange: CIG2. Purple: CIG3. Green: CIG4.

- [3] L. Sun, K. Sun, Y. Hou, and J. Hu, "Optimized autonomous operation control to maintain the frequency, voltage and accurate power sharing for DGs in islanded systems," *IEEE Transactions on Smart Grid*, vol. 11, no. 5, pp. 3885–3895, Sep. 2020.
- [4] Y. Zhu, F. Zhuo, F. Wang, B. Liu, R. Gou, and Y. Zhao, "A virtual impedance optimization method for reactive power sharing in networked microgrid," *IEEE Transactions on Power Electronics*, vol. 31, no. 4, pp. 2890–2904, April 2016.
- [5] C.-T. Lee, C.-C. Chu, and P.-T. Cheng, "A new droop control method for the autonomous operation of distributed energy resource interface converters," *IEEE Transactions on Power Electronics*, vol. 28, no. 4, pp. 1980–1993, April 2013.
- [6] H. Zhang, S. Kim, Q. Sun, and J. Zhou, "Distributed adaptive virtual impedance control for accurate reactive power sharing based on consensus control in microgrids," *IEEE Transactions on Smart Grid*, vol. 8, no. 4, pp. 1749–1761, July 2017.
- [7] J. W. Simpson-Porco, Q. Shafiee, F. Dörfler, J. C. Vasquez, J. M. Guerrero, and F. Bullo, "Secondary frequency and voltage control of islanded microgrids via distributed averaging," *IEEE Transactions on Industrial Electronics*, vol. 62, no. 11, pp. 7025–7038, Nov 2015.
- [8] S. Shrivastava, B. Subudhi, and S. Das, "Voltage and frequency synchronization of a low voltage inverter based microgrid," in *2017 4th International Conference on Power, Control Embedded Systems (ICPCES)*, March 2017, pp. 1–6.
- [9] A. Bidram, A. Davoudi, F. L. Lewis, and J. M. Guerrero, "Distributed cooperative secondary control of microgrids using feedback linearization," *IEEE Transactions on Power Systems*, vol. 28, no. 3, pp. 3462–3470, Aug 2013.
- [10] A. Bidram, A. Davoudi, F. L. Lewis, and Z. Qu, "Secondary control of microgrids based on distributed cooperative control of multi-agent systems," *IET Generation, Transmission & Distribution*, vol. 7, no. 8, pp. 822–831, Aug 2013.
- [11] A. Bidram, F. L. Lewis, and A. Davoudi, "Distributed control systems for small-scale power networks: Using multiagent cooperative control theory," *IEEE Control Systems Magazine*, vol. 34, no. 6, pp. 56–77, Dec 2014.
- [12] N. Pogaku, M. Prodanovic, and T. C. Green, "Modeling, analysis and testing of autonomous operation of an inverter-based microgrid," *IEEE Transactions on Power Electronics*, vol. 22, no. 2, pp. 613–625, March 2007.
- [13] J. Rocabert, A. Luna, F. Blaabjerg, and P. Rodríguez, "Control of power converters in ac microgrids," *IEEE Transactions on Power Electronics*, vol. 27, no. 11, pp. 4734–4749, Nov 2012.
- [14] S. S. Kia, B. Van Scoy, J. Cortes, R. A. Freeman, K. M. Lynch, and S. Martinez, "Tutorial on dynamic average consensus: The problem, its applications, and the algorithms," *IEEE Control Systems Magazine*, vol. 39, no. 3, pp. 40–72, June 2019.